Journal of Computational Physics **164,** 81–103 (2000)
doi:10.1006/jcph.2000.6574, available online at http://www.idealibrary.com on IDEAL®

Spectral Element Methods for Axisymmetric Stokes Problems

M. I. Gerritsma* and T. N. Phillips†

*Delft University of Technology, Faculty of Aerospace Engineering, Kluyverweg 1, 2629 HS, Delft, The Netherlands; and † Department of Mathematics, University of Wales, Aberystwyth SY23 3BZ, United Kingdom
E-mail: M.I.Gerritsma@lr.tudelft.nl, tnp@aber.ac.uk

Received April 15, 1999; revised June 26, 2000

The approximation of the Stokes problem in axisymmetric geometries using the spectral element method is considered. The presence of the volume element $r\,dr\,dz$ in the weak formulation of the problem is shown to be a potential source of difficulty. The discrete equations associated with nodes on the axis of symmetry can lead to a degeneracy in the global system of equations. This difficulty is resolved by incorporating the factor r into the weight function for spectral elements adjacent to the axis of symmetry and using appropriate basis functions in these elements in the radial direction. Properties of the Jacobi polynomials are used to construct the elements of the modified method. Numerical results are presented demonstrating some of the features of the proposed approach.

Key Words: spectral methods; domain decomposition; axisymmetric problems; orthogonal polynomials.

1. INTRODUCTION

In the weak formulation of a system of partial differential equations defined in an axisymmetric geometry special attention needs to be paid to the discretization along the axis of symmetry due to the presence of r factors which originate from the definition of the infinitesimal volume $d\Omega = r\,dr\,dz$. On the axis of symmetry some of the equations generate trivial algebraic relations ($0 = 0$), which result in an underdetermined system of equations. It is possible to divide both sides of the offending equation by the radial distance, r, before taking the limit $r \to 0$. This method is, for instance, applied by Van Kemenade and Deville [9] to the integration of the extra-stress components along the centerline of an axisymmetric viscoelastic flow problem. However, in certain cases, the existence of a trivial equation depends on the orthogonality of the grid on the symmetry axis. This is, for instance, the case for the gradient of the pressure in the axial direction in flow problems.

0021-9991/00 $35.00

The use of Jacobi polynomials will be illustrated using the Stokes equations for an incompressible creeping flow. The Stokes equations in an axisymmetric coordinate system are given by the incompressibility constraint

$$\frac{1}{r}\frac{\partial(ru_r)}{\partial r} + \frac{\partial u_z}{\partial z} = 0, \tag{1}$$

the momentum equations

$$\frac{\partial p}{\partial r} = \frac{1}{r}\frac{\partial(r\tau_{rr})}{\partial r} + \frac{\partial \tau_{rz}}{\partial z} - \frac{\tau_{\theta\theta}}{r} \tag{2}$$

and

$$\frac{\partial p}{\partial z} = \frac{1}{r}\frac{\partial(r\tau_{rz})}{\partial r} + \frac{\partial \tau_{zz}}{\partial z}, \tag{3}$$

and the Newtonian constitutive equation

$$\begin{pmatrix} \tau_{rr} & \tau_{rz} & 0 \\ \tau_{rz} & \tau_{zz} & 0 \\ 0 & 0 & \tau_{\theta\theta} \end{pmatrix} = \eta \begin{pmatrix} 2\frac{\partial u_r}{\partial r} & \frac{\partial u_r}{\partial z} + \frac{\partial u_z}{\partial r} & 0 \\ \frac{\partial u_r}{\partial z} + \frac{\partial u_z}{\partial r} & 2\frac{\partial u_z}{\partial z} & 0 \\ 0 & 0 & 2\frac{u_r}{r} \end{pmatrix}, \tag{4}$$

in which $\mathbf{u} = (u_r, u_z)$ denotes the velocity vector in axisymmetric coordinates, p is the pressure, $\boldsymbol{\tau}$ is the extra-stress tensor, and η is the viscosity coefficient.

Consider the numerical solution of the Stokes problem in some axisymmetric geometry, Ω, using the spectral element method. The domain Ω is divided into a number of nonoverlapping spectral elements, Ω_k, $k = 1, \ldots, K$. Each spectral element Ω_k is mapped onto the parent element $D = [-1, 1] \times [-1, 1]$. The mapping is usually performed using an isoparametric or transfinite mapping. Therefore, we may associate with each point $(s, t) \in D$ a unique point $(r, z) \in \Omega_k$, i.e.,

$$r(s, t) = f(s, t), \quad z(s, t) = g(s, t),$$

where f and g are prescribed functions.

The $P_N - P_{N-2}$ method of Maday and Patera [7] ensures compatibility between the discrete velocity and pressure spaces. In this method the pressure approximation is chosen to be a polynomial of degree 2 lower than the corresponding velocity approximation. The pressure approximation can be expressed in terms of Lagrangian interpolating polynomials based on the interior Gauss–Lobatto Legendre nodes. The Legendre polynomials are usually chosen for solving the weak formulation of the problem because of the unit weight function associated with them. Therefore, for $(r, z) \in \Omega_k$ we can write (see [3], for example)

$$p_N^k(r, z) = \sum_{i=1}^{N-1}\sum_{j=1}^{N-1} p_{i,j}\tilde{h}_i(s)\tilde{h}_j(t),$$

where $\tilde{h}_i(s)$, $i = 1, \ldots, N-1$, are the Lagrangian interpolating polynomials defined on the interior Gauss–Lobatto Legendre points.

The weak formulation of the component of the momentum equation in the axial direction (3) over element Ω_k is

$$-\int_{\Omega_k}\left(\tau^{rz}\frac{\partial v}{\partial r}+\tau^{zz}\frac{\partial v}{\partial z}-p\frac{\partial v}{\partial z}\right)r\,dr\,dz=0, \tag{5}$$

where v is a test function associated with the axial component of the velocity. Transforming this to the parent element gives

$$\int_D\left[-\tau^{rz}\left(\frac{\partial z}{\partial t}\frac{\partial v}{\partial s}-\frac{\partial z}{\partial s}\frac{\partial v}{\partial t}\right)-\tau^{zz}\left(-\frac{\partial r}{\partial t}\frac{\partial v}{\partial s}+\frac{\partial r}{\partial s}\frac{\partial v}{\partial t}\right)+p\left(-\frac{\partial r}{\partial t}\frac{\partial v}{\partial s}+\frac{\partial r}{\partial s}\frac{\partial v}{\partial t}\right)\right]\mathrm{sgn}(J)r(s,t)\,ds\,dt=0,$$

in which J is the determinant of the transfinite mapping. If one substitutes the above apprximation for p into this equation and considers the test functions

$$v_{k,l}(s,t)=h_k(s)h_l(t),\quad k,l=0,\ldots,N,$$

in which

$$h_i(x_j)=\begin{cases}1 & \text{if } j=i,\\ 0 & \text{otherwise,}\end{cases} \tag{6}$$

where x_i, $i=0,\ldots,N$, are the Gauss–Lobatto points to be derived in Section 3, and one replaces the domain integral by a quadrature rule based on the Gauss–Lobatto points, one obtains the discretization of the pressure term as

$$\sum_{m=0}^{N}\sum_{n=0}^{N}\left[\sum_{i=1}^{N-1}\sum_{j=1}^{N-1}p_{i,j}\tilde{h}_i(s_m)\tilde{h}_j(t_n)\left(\frac{\partial r}{\partial s}h_k(s_m)h_l'(t_n)-\frac{\partial r}{\partial t}h_k'(s_m)h_l(t_n)\right)r(s_m,t_n)w_mw_n\right], \tag{7}$$

for $k,l=0,\ldots,N$ and in which w_m, $m=0,\ldots,N$, are the weights associated with the Gauss–Lobatto integration rule.

We assume, without loss of generality, that the side which corresponds to the symmetry axis $r=0$ is parametrized by $s=-1$ on the parent domain. If the grid is locally orthogonal to the symmetry line, i.e., $\partial r/\partial t=0$ at $s=-1$, then the integral approximated by (7) vanishes if a Gauss–Lobatto integration is used to approximate the integral. The expression (7) yields zero when $k=0$ and l is arbitrary, i.e., a point on the symmetry axis, because the second term vanishes owing to the fact that $\partial r/\partial t=0$ while the first term does not contribute because the only nonzero contribution, due to (6), occurs when $s_m=0$, in which case $r(s_m,t_n)=0$. So for $k=0$ the gradient matrix for the pressure will contain a line with only zeros. Since the incompressibility matrix is the transpose of the gradient matrix, the incompressibility matrix will have a column containing only zeros when $k=0$. The extra-stress component τ_{zz}, however, does not contribute to (5) no matter what the value of $\partial r/\partial t$ is. The shear stress component in (5) is set equal to zero at the axis of symmetry.

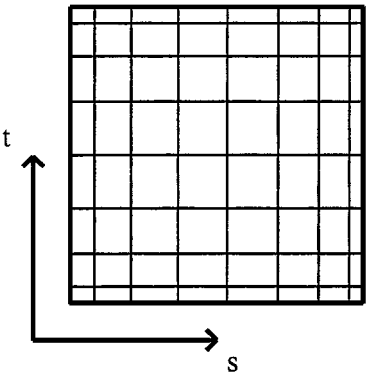

FIG. 1. Geometry of the parent domain for $N = 8$.

This, in itself, is a drawback of using Legendre basis functions in axisymmetric problems, but the situation deteriorates further if such an element is connected to a spectral element which is not orthogonal to the centerline, in which case the above integral does contribute to the discrete gradient operator, causing an artifical jump in the pressure solution along the centerline.

The main reason for this deficiency is that for points along the symmetry axis we have $r = 0$. This problem can be circumvented if the factor r is incorporated into the weight function provided, of course, that the numerical weights associated with this weight function can be shown to be positive. The classical orthogonal polynomials are all defined on the standard interval $[-1, 1]$. Therefore the continuous weight function which goes to zero in a similar fashion as r is given by $(1 + s)$, which is zero for $s = -1$. Comparing this with orthogonal polynomials arising from singular Sturm–Liouville problems leads us naturally to the Jacobi polynomials $P_k^{(\alpha,\beta)}(x)$ with $\alpha = 0$ and $\beta = 1$.

We will use these Jacobi polynomials only in the radial direction when the spectral element is adjacent to the centerline and retain the Legendre approximation in the axial direction. Figure 1 shows the parent domain and the Gauss–Lobatto grid in which in the s-direction (the vertical grid lines) a Jacobi–Gauss–Lobatto grid is used and in the t-direction (the horizontal grid lines) a Legendre–Gauss–Lobatto grid is used. If the spectral element is not adjacent to the symmetry line Legendre polynomials will be used in both directions. As can be seen from Fig. 1 the grid spacing on the Jacobi–Gauss–Lobatto grid is not symmetric in contrast to that on the Legendre grid.

The outline of the paper is as follows. In Section 2 the properties of the Jacobi polynomials that are relevant to this paper are presented. In Section 3 interpolating polynomials based on the Jacobi–Gauss–Lobatto are introduced together with associated quadrature rules. These polynomials are used as basis functions in the spectral element method. The source of difficulty along the axis of symmetry $r = 0$ is described in Section 4, and a technique, based on the introduction of a scaled radius $\tilde{r}$, which overcomes this problem is discussed. Finally, in Section 5 numerical results are presented for the application of the new approximation to the nontrivial axisymmetric problem of a sphere falling under the influence of gravity along the centerline of a cylindrical tube filled with a very viscous fluid. Section 6 concludes the paper with a summary of the result and a discussion of some of the issues raised. In the Appendix the corrected version of the subroutine `JACOBF` for the determination of the

Gauss–Lobatto integration points is given. The original version of this code can be found in [1].

2. JACOBI POLYNOMIALS

The Jacobi polynomials $P_k^{(\alpha,\beta)}(x)$ are the eigenfunctions of the Sturm–Liouville problem

$$-(p(x)u'(x))' + q(x)u(x) = \lambda w(x)u(x), \quad x \in (-1, 1), \tag{8}$$

together with suitable boundary conditions. The coefficients $p(x)$, $q(x)$, and $w(x)$ are real-valued functions such that $p(x)$ is a strictly positive, continuously differentiable function on $(-1, 1)$ and continuous at $x = \pm 1$; $q(x)$ is nonnegative, continuous, and bounded on $(-1, 1)$; and $w(x)$ is nonnegative, continuous, and integrable over $(-1, 1)$.

The Sturm–Liouville problem is singular if $p(x)$ vanishes at $x = \pm 1$. This property ensures that the expansion of an infinitely differentiable function in terms of these eigenfunctions converges with spectral accuracy; i.e., the coefficients with respect to this basis of eigenfunctions decay faster than algebraically. The Jacobi polynomials $P_k^{(\alpha,\beta)}(x)$ are the eigenfunctions of the singular Sturm–Liouville problem with

$$p(x) = (1 - x)^{1+\alpha}(1 + x)^{1+\beta}, \quad \text{for } \alpha, \beta > -1,$$
$$q(x) = 0,$$

and

$$w(x) = (1 - x)^{\alpha}(1 + x)^{\beta}.$$

Important special cases are obtained for $\alpha = \beta = 0$ (the Legendre polynomials) and for $\alpha = \beta = -1/2$ (the Chebyshev polynomials). The Jacobi polynomials satisfy the orthogonality property

$$\int_{-1}^{1} P_m^{(\alpha,\beta)}(x) P_n^{(\alpha,\beta)}(x) w(x)\, dx = 0, \quad \text{for } m \neq n.$$

The Jacobi polynomials may be generated efficiently using a three-term recurrence relation provided $P_0^{(\alpha,\beta)}(x)$ and $P_1^{(\alpha,\beta)}(x)$ are known. It is conventional to choose $P_0^{(\alpha,\beta)}(x) = 1$ and to construct $P_1^{(\alpha,\beta)}(x)$ using the above orthogonality relation. In addition the normalization condition $P_k^{(\alpha,\beta)}(1) = 1$, $\forall k$, is used. Thus, for $\alpha = 0$ and $\beta = 1$ we have

$$P_1^{(0,1)}(x) = \frac{1}{2}(3x - 1).$$

The particular values $\alpha = 0$ and $\beta = 1$ were chosen because this choice corresponds to a weight function $(1 + x)$ in the Sturm–Liouville problem. This particular weight function goes to zero for $x \to -1$ as $r \to 0$, as was explained in the introduction.

The corresponding eigenvalue is $\lambda_1 = 3$, which is obtained from (8).

Thus, with a knowledge of the first two members of the orthogonal set the remainder may be generated using the recurrence relation

$$P_{k+1}^{(0,1)}(x) = \left[\frac{(2k + 3)(2k + 1)x - 1}{(k + 2)(2k + 1)}\right] P_k^{(0,1)}(x) - \left[\frac{k(2k + 3)}{(k + 2)(2k + 1)}\right] P_{k-1}^{(0,1)}(x). \tag{9}$$

The proof of this recursion relation can be found in Szëgo [8] for general Jacobi polynomials. From (9) the recursion relation for the derivatives can be obtained:

$$\frac{d}{dx}P_{k+1}^{(0,1)}(x) = \left[\frac{2k+3}{k+2}\right]P_k^{(0,1)}(x) + \left[\frac{(2k+3)(2k+1)x-1}{(k+2)(2k+1)}\right]\frac{d}{dx}P_k^{(0,1)}(x) - \left[\frac{k(2k+3)}{(k+2)(2k+1)}\right]\frac{d}{dx}P_{k-1}^{(0,1)}(x). \tag{10}$$

The orthogonal polynomials generated by (9) all satisfy $P_k^{(0,1)}(1) = 1$. Further useful properties of the $P_k^{(0,1)}$ are listed below.

The corresponding eigenvalues are given by $\lambda_k = k(k+2)$. This follows immediately if one inserts a series $\sum_{i=0}^{\infty} a_i x^i$ and requires that all coefficients $a_l = 0$ for $l > k$. Therefore, the differential equation satisfied by the Jacobi polynomials $P_k^{(\alpha,\beta)}(x)$ can be written in the form

$$(1-x^2)\frac{d^2P_k^{(0,1)}}{dx^2} + (1-3x)\frac{dP_k^{(0,1)}}{dx} + k(k+2)P_k^{(0,1)} = 0. \tag{11}$$

Furthermore, we can establish by induction using (9) that

$$P_k^{(0,1)}(-1) = (-1)^k(k+1). \tag{12}$$

Since we know the values of $P_k^{(0,1)}(-1)$ and $P_k^{(0,1)}(1)$ we can use (11) to obtain expressions for the values of the derivative of $P_k^{(\alpha,\beta)}(x)$ at the end-points of the interval $[-1, 1]$:

$$\left.\frac{dP_k^{(0,1)}}{dx}\right|_{x=-1} = (-1)^{k+1}\frac{1}{4}k(k+1)(k+2) \tag{13}$$

and

$$\left.\frac{dP_k^{(0,1)}}{dx}\right|_{x=1} = \frac{1}{2}k(k+2). \tag{14}$$

Note that these particular Jacobi polynomials are neither symmetric nor antisymmetric, in contrast to the Legendre or Chebyshev polynomials.

3. REPRESENTATION OF THE BASIS FUNCTIONS IN THE RADIAL DIRECTION

Since the weak formulation of partial differential equations requires the evaluation of integrals a suitable integration method has to be selected. In this paper the Gauss–Lobatto integration method will be used. The integration points are given by the $(N+1)$ so-called Jacobi–Gauss–Lobatto points. The integration rule

$$\int_{-1}^{1} w(x)q(x)\,dx = \sum_{j=0}^{N} w_j q(x_j) \tag{15}$$

is exact for all polynomials $q(x)$ of degree $2N-1$ or less if the weights w_j, $j = 0, \ldots, N$,

satisfy the linear system of equations

$$\sum_{j=0}^{N}(x_j)^k w_j = \int_{-1}^{1} w(x)x^k\,dx, \quad 0 \le k \le N,$$

where $w(x)$ is the Sturm–Liouville weight function and the nodes x_j, $j = 0, 1, \ldots, N$, are chosen as follows: $x_0 = -1$, $x_N = 1$, and x_j, $j = 1, \ldots, N-1$, are the zeros of $dP_N^{(0,1)}/dx$. It is fairly straightforward to prove that all the Gauss–Lobatto points are contained in the interval $(-1, 1)$. The zeros of $dP_N^{(0,1)}/dx$ are usually calculated numerically using, for instance, the subroutine given in Appendix C of [1]. Since this subroutine contains a small error, a corrected version will be given in the Appendix. The associated weights in the numerical integration procedure for $\alpha = 0$, $\beta = 1$ are given by Funaro [2] as

$$w_0 = \frac{4(2N+1)}{N^2(N+1)^2(N-1)(N+2)}\sum_{j=1}^{N-1}(1-x_j),$$

$$w_j = -\frac{2(2N+1)}{N(N+2)}\cdot\frac{1}{P_N^{(0,1)}(x_j)\frac{d}{dx}P_{N-1}^{(0,1)}(x_j)}, \quad 1 \le j \le N-1,$$

$$w_N = \frac{2(2N+1)}{(N+2)(N+1)N(N-1)}\sum_{j=1}^{N-1}(1+x_j),$$

where x_j, $1 \le j \le N-1$, are the interior Gauss–Lobatto points. The values of $P_N^{(0,1)}(x_j)$ and $dP_{N-1}^{(0,1)}(x_j)/dx$ can be determined using the recursion relations (9) and (10), respectively.

Instead of expanding a function in terms of orthogonal polynomials directly, one usually prefers to approximate the function using a Lagrangian interpolating polynomial based on the Gauss–Lobatto points. Therefore, in the present situation the polynomial $I_N u$ which interpolates a given function u at the Gauss–Lobatto points has the representation

$$(I_N u)(x) = \sum_{j=0}^{N} u_j h_j(x), \tag{16}$$

where the Lagrangian coefficients are given by

$$h_0(x) = \frac{2(-1)^N(x-1)\left[\frac{d}{dx}P_N^{(0,1)}(x)\right]}{(N+2)(N+1)N}, \tag{17}$$

$$h_j(x) = \frac{(x^2-1)\left[\frac{d}{dx}P_N^{(0,1)}(x)\right]}{N(N+2)P_N^{(0,1)}(x_j)(x-x_j)}, \quad 1 \le j \le N-1, \tag{18}$$

$$h_N(x) = \frac{(x+1)\left[\frac{d}{dx}P_N^{(0,1)}(x)\right]}{N(N+2)}. \tag{19}$$

The polynomials $h_i(x)$ are constructed so that $h_i(x_j) = \delta_{ij}$. The derivative of the interpolant at the nodes may be computed using

$$(I_N u)'(x_i) = \sum_{j=0}^{N} D_{i,j}u_j, \tag{20}$$

where $D_{ij} = h'_j(x_i)$. Using (17)–(19) one can obtain explicit representations of the elements of D given by

$$D_{i,j} = \begin{cases} \frac{-N(N+2)}{6}, & i = j = 0, \\ \frac{2(-1)^N}{(N+1)} \frac{P_N^{(0,1)}(x_i)}{(1+x_i)}, & 1 \le i \le N-1,\ j = 0, \\ \frac{(-1)^N}{(N+1)}, & i = N,\ j = 0, \\ \frac{(-1)^N N}{2} \cdot \frac{1}{P_N^{(0,1)}(x_j)(1+x_j)}, & i = 0,\ 1 \le j \le N-1, \\ \frac{P_N^{(0,1)}(x_i)}{P_N^{(0,1)}(x_j)} \frac{1}{(x_i - x_j)}, & i \ne j,\ 1 \le i, j \le N-1, \\ \frac{-1}{2(1+x_i)}, & 1 \le i = j \le N-1, \\ \frac{1}{P_N^{(0,1)}(x_j)} \cdot \frac{1}{(1-x_j)}, & i = N,\ 1 \le j \le N-1, \\ \frac{(-1)^{(N+1)}}{4}(N+1), & i = 0,\ j = N, \\ \frac{-P_N^{(0,1)}(x_i)}{(1-x_i)}, & 1 \le i \le N-1,\ j = N, \\ \frac{N(N+2)-1}{4}, & i = j = N. \end{cases} \tag{21}$$

4. DISCRETIZATION ON THE AXIS OF SYMMETRY

Consider the weak form of the (partial differential) equation $Lu = f$ in an axisymmetric coordinate system. Suppose $u \in \mathcal{V}$ is approximated by $u^h \in \mathcal{V}^h$. The weak formulation of this axisymmetric problem is: Find $u^h \in V^h$ such that

$$\int_r \int_z (Lu^h, v^h)\, r\, dr\, dz = \int_r \int_z f v^h r\, dr\, dz \quad \forall v^h \in \mathcal{V}^h, \tag{22}$$

in which both r and z are functions of s and t defined on the parent element. Rewriting this in terms of the Jacobi polynomials with weight function $w(s) = (1+s)$ gives

$$\int_r \int_z (Lu^h, v^h) \frac{r}{w}\, w\, dr\, dz = \int_r \int_z f v^h \frac{r}{w} w\, dr\, dz \quad \forall v^h \in \mathcal{V}^h. \tag{23}$$

If one now lets $s \to -1$ then both $r \to 0$ and $w \to 0$; therefore r/w is given by L'Hôpital's rule by

$$\frac{r}{w} = \frac{r(s,t)}{(1+s)} = \left.\frac{\partial r}{\partial s}\right|_{s=-1} \quad \text{if } s = -1. \tag{24}$$

The multiplicative factor w in the weak formulation is absorbed into the numerical weights and these are always positive, even at the centerline. It is therefore convenient to introduce the scaled radius $\tilde{r}$ by

$$\tilde{r} = \begin{cases} \frac{r}{w} & \text{if } r > 0, \\ \frac{\partial r}{\partial s} & \text{if } r = 0. \end{cases} \tag{25}$$

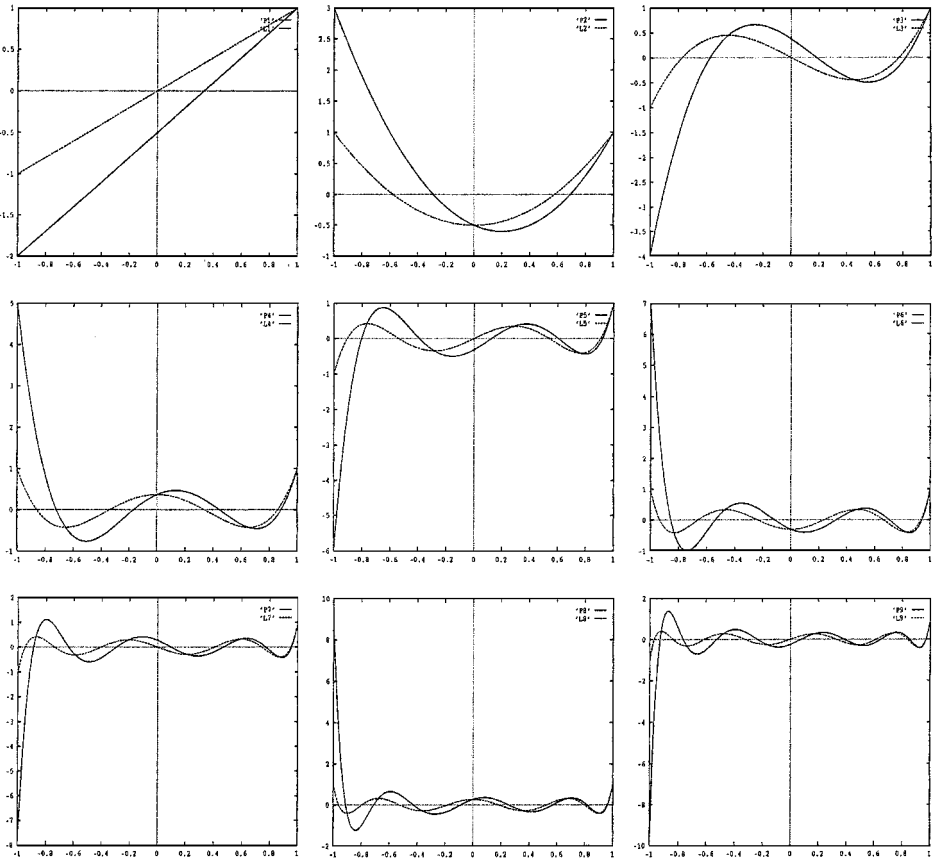

FIG. 2. Comparison between the Jacobi polynomials (dotted curve) and the Legendre polynomials (solid curve) for $N = 1, \ldots, 9$.

Note that $\partial r/\partial s \neq 0$ so the trivial equation mentioned in the introduction is circumvented. Furthermore the scaling of r can be performed beforehand without testing whether we are really dealing with a "$0 = 0$" equation or not.

Since we want to connect spectral elements adjacent to the symmetry axis in which the function is described by Jacobi polynomials with spectral elements not adjacent to the symmetry axis in which the solution in the radial direction is described by Legendre polynomials it is instructive to see how the Jacobi polynomials behave for $s \to 1$. Figure 2 compares the first nine Jacobi polynomials with the corresponding Legendre polynomials. This figure demonstrates that when N increases the behavior of both polynomials near $s = 1$ coincides. This also follows from the fact that $P_N^{(0,1)}(1) = P_N^{(0,0)}(1) = 1$ and that

$$\left.\frac{d}{dx} P_N^{(0,0)}\right|_{x=1} = \frac{1}{2} N(N+1),$$

while

$$\left.\frac{d}{dx} P_N^{(0,1)}\right|_{x=1} = \frac{1}{2} N(N+2),$$

so

$$\left.\frac{d}{dx}P_N^{(0,1)}\right|_{x=1} \to \left.\frac{d}{dx}P_N^{(0,0)}\right|_{x=1} \quad \text{for } N \to \infty.$$

5. THE SPHERE IN A TUBE

The method described in the preceding section will now be applied to the mixed velocity–pressure–stress formulation of the Stokes problem. Existence and uniqueness of this mixed method have been discussed in [3, 4].

The velocity–pressure–stress formulation of the Stokes problem involves the solution of the following system of partial differential equations:

$$\begin{aligned} \boldsymbol{\tau} - 2\eta \boldsymbol{d} &= 0, \\ \boldsymbol{\nabla} \cdot \boldsymbol{\tau} - \boldsymbol{\nabla} p &= 0, \\ \boldsymbol{\nabla} \cdot \mathbf{w} &= 0. \end{aligned} \tag{26}$$

Here $\boldsymbol{\tau}$ is the extra-stress tensor, $\mathbf{w}$ is the velocity, p is the pressure, and $\boldsymbol{d}$ is the rate of deformation tensor. The constant η is the kinematic viscosity.

The configuration considered is a sphere with radius R_s falling along the centerline of a tube of radius R_t with a prescribed velocity V. This situation is sketched in Fig. 3. The idea is to divide the physical domain Ω into several spectral elements, Ω_k, $1 \le k \le K$, such

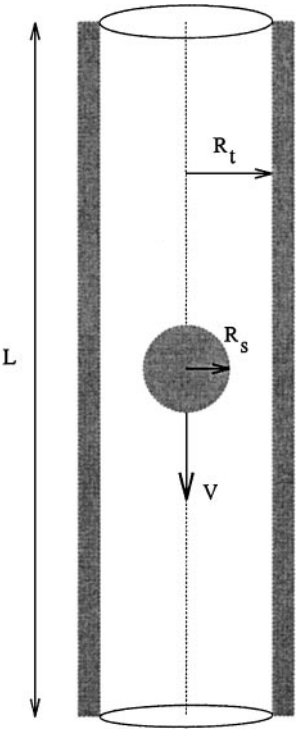

FIG. 3. Geometry of the sphere in a tube.

that $\bigcup_{k=1}^{K} \bar{\Omega}_k = \bar{\Omega}$ and $\Omega_k \cap \Omega_l = \emptyset$ for all $k \neq l$. We also assume that the decomposition is geometrically conforming in the sense that the intersection of two adjacent elements is either a common vertex or an entire edge. Each of the spectral elements is mapped onto the parent element $D = [-1, 1] \times [-1, 1]$ using the transfinite mapping technique [5]. Note that when a bilinear transfinite mapping is used, the grid can be only C^0 across element boundaries.

We approximate the dependent variables on the parent element using Legendre Lagrangian interpolants of degree N in both spatial directions or, when the spectral element is adjacent to the symmetry line, Jacobi Lagrangian interpolants in the radial direction only. Let $P_{N,K}(\Omega)$ denote the space of polynomials of degree N or less, defined over the K elements. We choose the velocity field in $P_{N,K}(\Omega) \cap H^1(\Omega)$ and construct a Gauss–Lobatto Legendre grid in each of the elements Ω_k, $1 \leq k \leq K$. The choice of velocity approximation space ensures that continuity is enforced across element boundaries. The velocity representation is then given by

$$\mathbf{v}_N^k(\xi, \zeta) = \sum_{i=0}^{N} \sum_{j=0}^{N} \mathbf{v}_{i,j}^k h_i(\xi) h_j(\zeta), \tag{27}$$

where the Lagrangian interpolants $h_i(\xi)$, $0 \leq i \leq N$, defined on the parent interval with $\xi \in [-1, 1]$, are given either by the Legendre Lagrangian interpolant

$$h_i(\xi) = -\frac{(1 - \xi^2) L'_N(\xi)}{N(N+1) L_N(\xi_i)(\xi - \xi_i)} \tag{28}$$

or by the Jacobi Lagrangian interpolant given by (17)–(19).

Maday and Patera [7] have shown that by choosing $P_{N-2}(\Omega)$ as the approximation space for the pressure if the velocity approximation space is $P_N(\Omega)$ the discrete Babuška–Brezzi condition is satisfied. For the Legendre approximation this means that the pressure is expanded as

$$p_N^k(\xi, \zeta) = \sum_{i=1}^{N-1} \sum_{j=1}^{N-1} p_{i,j} \tilde{h}_i(\xi) \tilde{h}_j(\zeta), \tag{29}$$

in which the interpolants $\tilde{h}_i(\xi)$, $1 \leq i \leq N-1$, are defined on the interval $[-1, 1]$ and in the case of the Legendre polynomials are given by

$$\tilde{h}_i(\xi) = -\frac{\left(1 - \xi_i^2\right) L'_N(\xi)}{N(N+1) L_N(\xi_i)(\xi - \xi_i)} \tag{30}$$

and for the Jacobi polynomials are given by

$$\tilde{h}_i(\xi) = -\frac{\left(1 - \xi_i^2\right) \left[\frac{d}{d\xi} P_N^{(0,1)}(\xi)\right]}{N(N+2) P_N^{(0,1)}(\xi_i)(\xi - \xi_i)}. \tag{31}$$

The components of the extra-stress tensor are chosen in $P_{N,K}(\Omega)$. This means that the extra-stress tensor has a representation of the form

$$\boldsymbol{\tau}_N^k(\xi, \zeta) = \sum_{i=0}^{N} \sum_{j=0}^{N} \boldsymbol{\tau}_{i,j}^k h_i(\xi) h_j(\zeta), \tag{32}$$

in which $h_i(\xi)$ is given either by (28) for the Legendre polynomials or by (17)–(19) for the Jacobi polynomials.

Along an element interface contiguous elements share common grid points and so there are two unknowns associated with each component of velocity and extra-stress at such points. The values of these unknowns are forced to be the same for the velocity, thus giving rise to a continuous velocity approximation. However, this is not done explicitly for the extra-stress, which therefore allows for the possibility of a discontinuous extra-stress approximation across element boundaries (see [4] for the justification of this approach).

The discrete problem is constructed by choosing appropriate test spaces for each of the variables and then using a basis for these spaces as test functions in the variational formulation. This process leads to the system

$$\begin{aligned} A_N \boldsymbol{\tau}_N - B_N^* \mathbf{w}_N &= \boldsymbol{f}_N, \\ -B_N \boldsymbol{\tau}_N + D_N^* p_N &= \mathbf{g}_N, \\ D_N \mathbf{w}_N &= h_N, \end{aligned} \tag{33}$$

in which $\boldsymbol{f}_N$ contains Dirichlet boundary conditions and the body forces, $\mathbf{g}_N$ contains prescribed boundary values, and h_N contains prescribed velocity values. Here A_N is the extra-stress mass matrix, B_N is the spectral approximation to the divergence operator acting on symmetric 2-tensors, and D_N is the spectral approximation of the divergence operator acting on vectors.

This system of equations can be written more succinctly as

$$\begin{pmatrix} A_N & -B_N^* & 0 \\ -B_N & 0 & D_N^* \\ 0 & D_N & 0 \end{pmatrix} \begin{pmatrix} \boldsymbol{\tau}_N \\ \mathbf{w}_N \\ p_N \end{pmatrix} = \begin{pmatrix} \boldsymbol{f}_N \\ \mathbf{g}_N \\ h_N \end{pmatrix}. \tag{34}$$

Since A_N is a diagonal matrix, owing to the orthogonality of the basis functions, (34) constitutes a symmetric system. The zeros on the diagonal of this system mean that either pivoting or preconditioning is required to solve it numerically. Following the doubly constrained minimization procedure described in [3] this system can be solved. This approach essentially applies pivoting and an incomplete LU-factorization.

Eliminating the discrete extra-stress tensor from (33^1) and (33^2) one obtains

$$-B_N A_N^{-1} B_N^* \mathbf{w}_N + D_N^* p_N = \mathbf{g}_N + B_N A_N^{-1} \boldsymbol{f}_N. \tag{35}$$

Since the mass matrix, A_N, is a diagonal matrix with strictly positive diagonal elements, (35) can be set up using $\sim N^{3d}/2$ multiplications, in which N is the polynomial order used in the spectral method, d is the number of spatial dimensions, and the factor $1/2$ is obtained if one takes the symmetry of $-B_N A_N^{-1} B_N^*$ into account. This matrix, however, does not have to be formed explicitly if an iterative solution method is used since one only needs to calculate the operation of this matrix on a given vector.

Eliminating the discrete velocity vector $\mathbf{w}_N$ from (35) and (33^3) yields the equation which p_N has to satisfy for $\mathbf{w}_N$ to satisfy (33),

$$Q_N p_N = h_N - D_N \left(B_N A_N^{-1} B_N^*\right)^{-1} \left(\mathbf{g}_N + B_N A_N^{-1} \boldsymbol{f}_N\right), \tag{36}$$

where

$$Q_N = -D_N \left(B_N A_N^{-1} B_N^* \right)^{-1} D_N^*. \tag{37}$$

Although $B_N A_N^{-1} B_N^*$ is a full matrix its inverse does not need to be calculated when a nested conjugate gradient (CG) method is used to solve (36) for p_N.

Once p_N is calculated from (36), the vector $\mathbf{w}_N$ satisfying (33^3) can be calculated from (35), after which the discrete extra-stress approximation $\boldsymbol{\tau}_N$ which will satisfy (33^2) follows from (33^1). So the whole solution procedure follows the same doubly constrained approach as the compatibility analysis described in [3].

The physical parameters used in the problem of flow past a sphere are $V = 1$, $\eta = 1$, $R_s = 1$, $R_t = 2$, and $L = 8$. This means that the velocity is zero at the sphere and $u_z = 1$, $u_r = 0$ at inflow, outflow, and the cylinder wall. At the axis of symmetry $u_r = 0$ and $\tau_{rz} = 0$. Although the presence of the sphere is felt everywhere in the cylinder due to the elliptic nature of the governing equations, a cylinder of length $L = 8$ is sufficient to calculate the nondimensional drag. The discretization parameter is N, the degree of the spectral approximation in each element. Results obtained on the nearly orthogonal meshes depicted in Fig. 4 are presented using $N = 6, 8, 10$, and 12 for the Jacobi–Legendre method. These plots indicate that no spurious transitions from Jacobi–Legendre elements to Legendre–Legendre elements are present. Also, the solution at and near the symmetry axis is well resolved using the mixed Jacobi–Legendre interpolation.

Figure 5 presents a sequence of meshes that are nonorthogonal to the symmetry axis. Figure 6 displays the contour plot of the pressure for $N = 10$. The behavior of the extra-stress components and their dependence on the value of N along the symmetry axis and

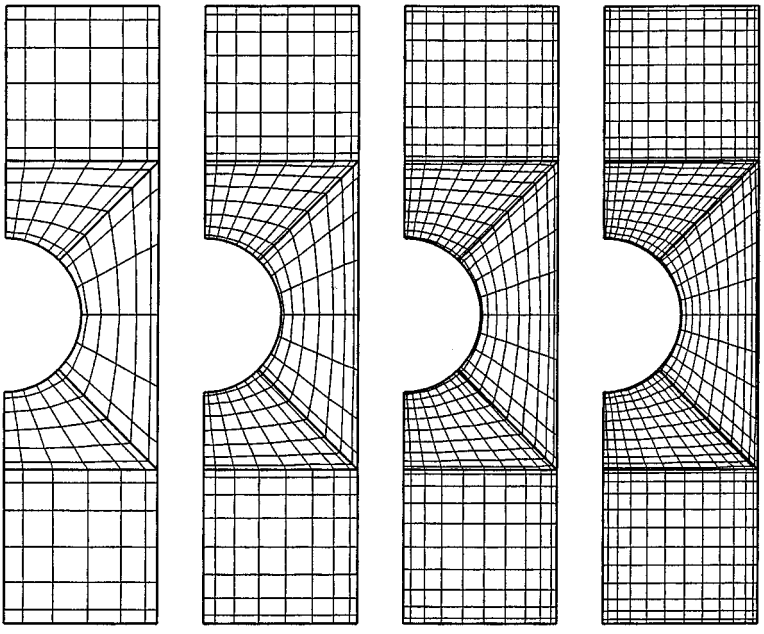

FIG. 4. The four spectral element grids for which results of the sphere–cylinder problem are given. These correspond to $N = 6$, $N = 8$, $N = 10$, and $N = 12$, respectively for $K = 5$. The bold lines indicate the spectral elements; the other lines are the Gauss–Lobatto grid. This mesh is nearly orthogonal to the symmetry axis.

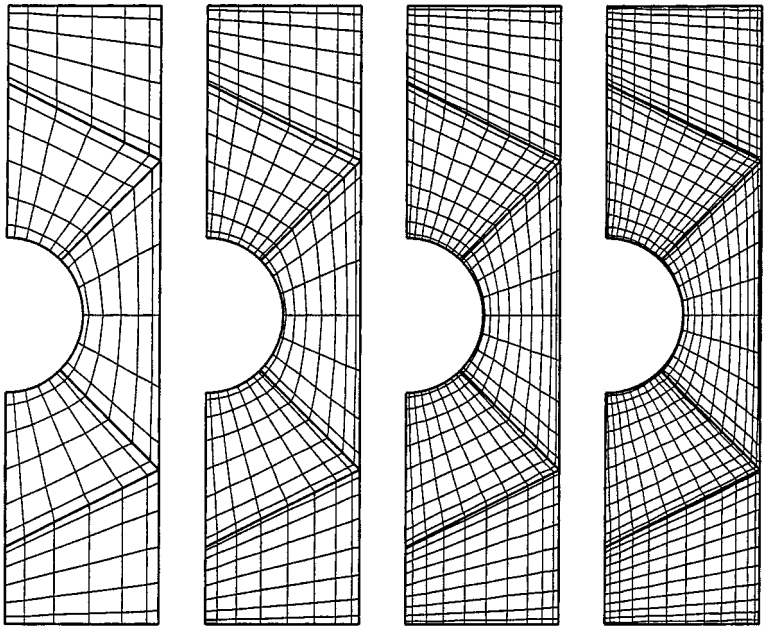

FIG. 5. The four spectral element grids for which results of the sphere–cylinder problem are given. These correspond to $N = 6$, $N = 8$, $N = 10$, and $N = 12$, respectively for $K = 5$. The bold lines indicate the spectral elements; the other lines are the Gauss–Lobatto grid. This mesh is nonorthogonal to the symmetry axis.

the sphere are given in Figs. 7–10 for $N = 6$, 8, and 10. All solutions are interpolated on a fine mesh with polynomials of order $N = 20$ before plotting. Since the graphs for $N = 8$ and $N = 10$ are almost indistinguishable, there was little point in increasing the degree of approximation further. All the graphs show that convergence has been obtained for points

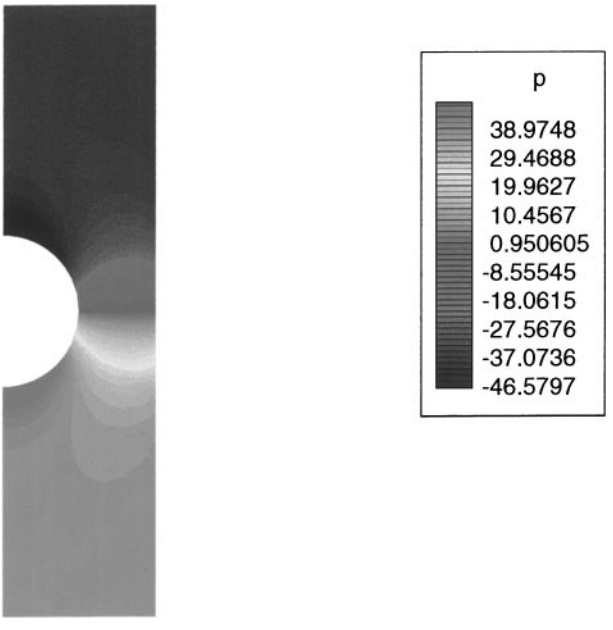

FIG. 6. Contour plot of the pressure.

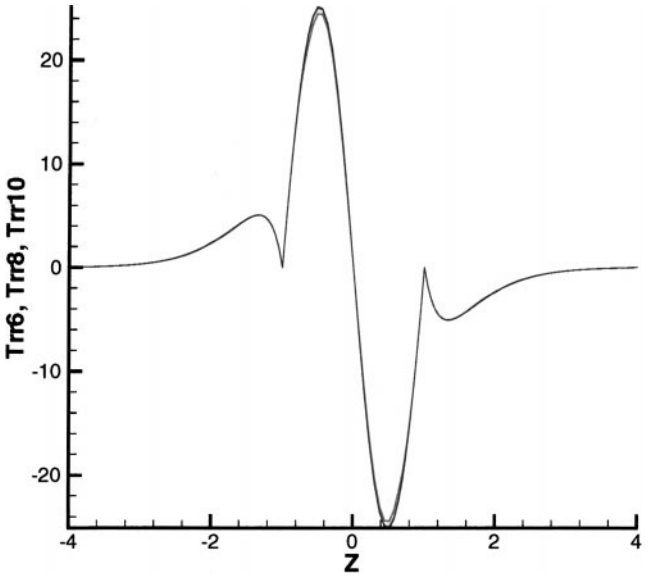

FIG. 7. Graphs of the extra-stress component τ_{rr} along the symmetry axis and the sphere for $N = 6$, $N = 8$, and $N = 10$.

on the symmetry axis. The only differences occur for points on the surface of the sphere, which also explains the different nondimensional drags for various polynomial orders given in Table I.

The graph of the τ_{zz}-component of the extra-stress tensor depicted in Fig. 9 for $N = 6$ shows little bumps near $x = -2$ and $x = 2$. These are a result of the discontinuous

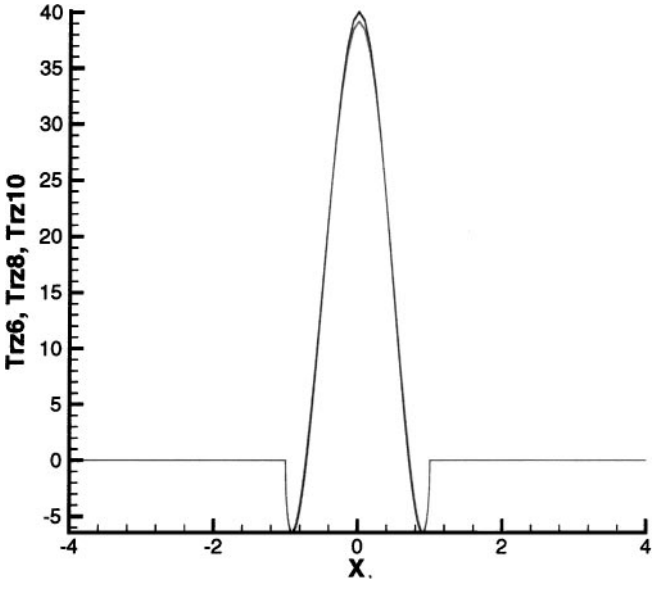

FIG. 8. Graphs of the extra-stress component τ_{rz} along the symmetry axis and the sphere for $N = 6$, $N = 8$, and $N = 10$.

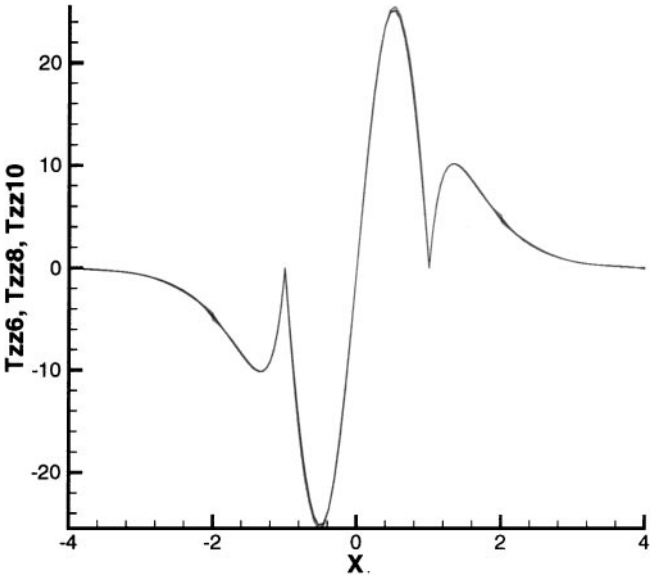

FIG. 9. Graphs of the extra-stress component, τ_{zz} along the symmetry axis and the sphere for $N = 6$, $N = 8$, and $N = 10$.

L^2-approximation of the extra-stress components as explained in [4]. For higher values of N this jump decreases and will vanish in the limit of $N \to \infty$.

The pressure along the symmetry axis, which was identified in the introduction as a potential source of difficulty, is displayed in Fig. 11. Since the pressure is determined up to a constant the graphs for different values of N do not necessarily overlap. To compare the

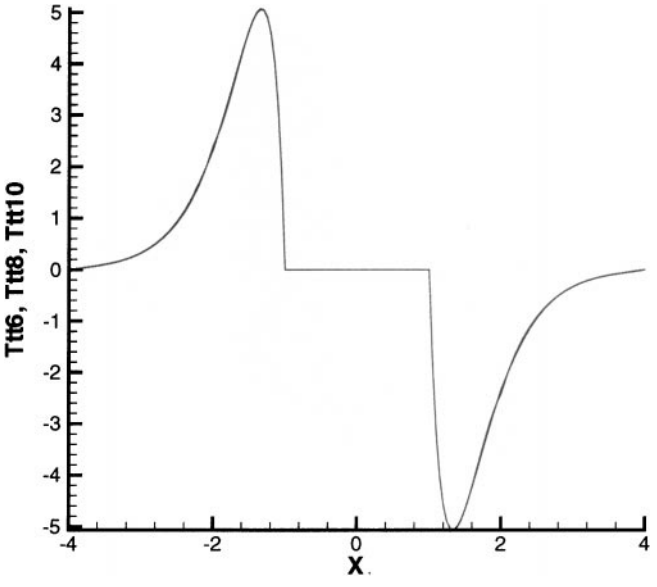

FIG. 10. Graphs of the extra-stress component $\tau_{\theta\theta}$ along the symmetry axis and the sphere for $N = 6$, $N = 8$, and $N = 10$.

TABLE I

Nondimensionalized Drag on the Sphere Calculated with the Jacobi–Legendre Method and the Legendre–Legendre Method on a Nearly Orthogonal Mesh

N	F^* Legendre–Legendre	F^* Jacobi–Legendre
6	5.949195	5.945073
8	5.948211	5.949030
10	5.947920	5.947822
12	5.947471	5.947394
14	5.947388	—
16	5.947381	—
18	5.947381	—

Note. Drag compared to $F^* = 5.94739$.

various approximations, the pressure level has been chosen such that the pressure is equal to zero for $x = 0$. The inset to Fig. 11 shows the convergence of the pressure jump between spectral elements for increasing polynomial order.

A nondimensional quantity which is widely used to demonstrate convergence of a given numerical method on the sphere problem is the drag on the sphere. This is defined to be the drag on the sphere divided by the Stokes drag of a sphere in an infinite expanse, $D = 6\pi\eta R_s V$. These results are tabulated in Table I. The nondimensionalized drag coefficients are compared with the value obtained by [6] on their finest mesh using the EEME/FEM.

The results in Table I are compared with more extensive computations using the Legendre–Legendre formulation. Both methods display an exponential convergence toward the limiting value of $F^* = 5.9474$, in accordance with the results by Lunsmann *et al.* [6]. Table I shows that the new polynomial basis is able to give results comparable with a method which also produces satisfactory results. This is a prerequisite for any new method!

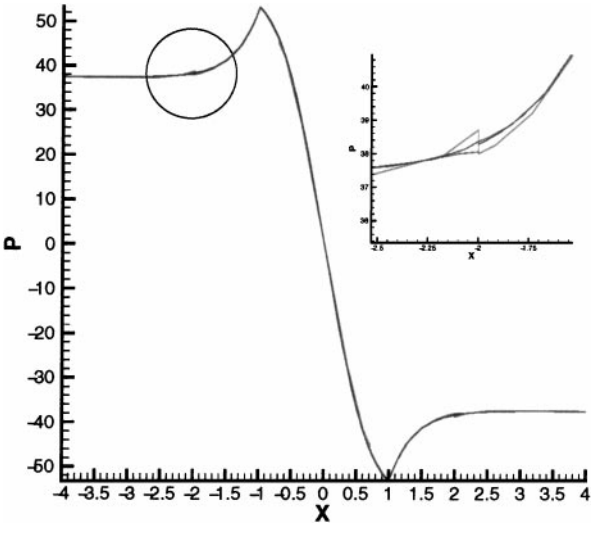

FIG. 11. Graphs of the pressure p along the symmetry axis and the sphere for $N = 6$, $N = 8$, and $N = 10$.

TABLE II

Nondimensionalized Drag on the Sphere Calculated with the Jacobi–Legendre Method and the Legendre–Legendre Method on a Skew Mesh

N	F^* Legendre–Legendre	F^* Jacobi–Legendre
6	5.963221	5.954784
8	5.955422	5.950952
10	5.950300	5.948051
12	5.948018	5.947435

Note. Drag compared to $F^* = 5.94739$.

Similar calculations have been performed on the meshes displayed in Fig. 5 (see Table II). Again all meshes consist of five spectral elements with increasing polynomial order. Although the solutions on both meshes converge to the limiting value of $F^* = 5.9474$ the Jacobi–Legendre formulation gives a slightly smaller error than does the conventional Legendre–Legendre approach. This means that the Jacobi–Legendre basis offers an improvement over the Legendre–Legendre formulation in this specific case. However, it is not clear whether this conclusion holds in general. We expect that the differences between the Jacobi–Legendre and the Legendre–Legendre method are small in situations where the grid is almost orthogonal to the axis of symmetry but that the Jacobi–Legendre performs better in the case where the grid lines are nonorthogonal to the symmetry axis. This is graphically illustrated by Figs. 12 and 13. For the case where the grid lines are almost normal to the axis of symmetry both logarithmic errors are of the same order of magnitude. Figure 12 seems to suggest that the Jacobi–Legendre method converges faster for higher N, than does the Legendre–Legendre method, but the values of N are too low to actually conclude this.

Figure 13 shows that in the case where the grid lines are highly nonorthogonal to the symmetry axis the logarithmic error as a function of N is much smaller for the Jacobi–Legendre method than for the Legendre–Legendre method as was anticipated in the discussion in Section 1.

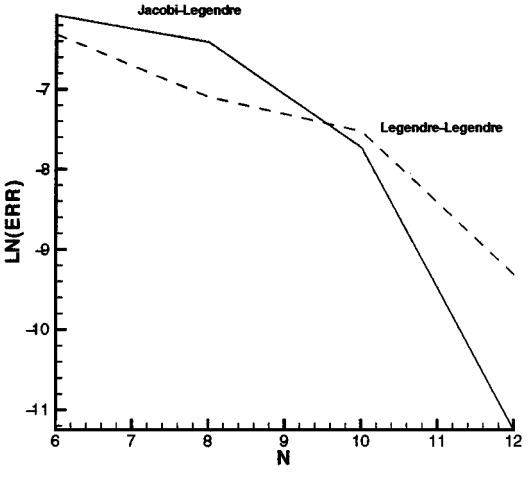

FIG. 12. Logarithmic convergence plot corresponding to the data in Table I.

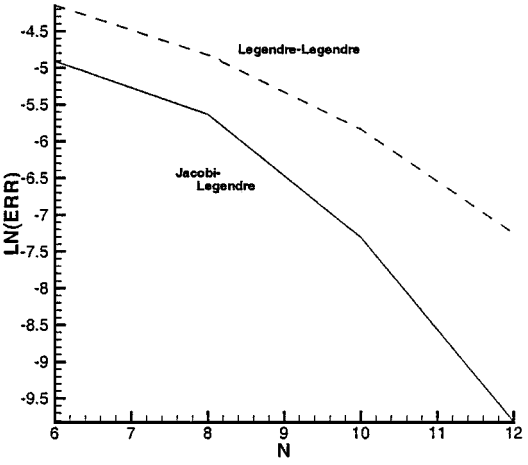

FIG. 13. Logarithmic convergence plot corresponding to the data in Table II.

6. CONCLUSIONS

The use of Jacobi polynomials in spectral elements adjacent to the axis of symmetry in axisymmetric problems circumvents a special treatment for points for which $r = 0$ by introducing a scaled radial distance $\tilde{r}$. This means that one does not have to check whether one is dealing with a trivial equation since the scaled radial distance can be introduced beforehand. This in itself is a special treatment, but it is automatically built into the method. By using the Jacobi polynomials in the Stokes problem discussed above, we see that the axial pressure gradient along the centerline contributes to the set of algebraic equations to be solved, whereas if Legendre polynomials were used this would not, in general, have been the case. A comparison with the Legendre–Legendre formulation, in which the trivial equation is avoided by means of an application of L'Hôpital's rule, shows an exponential rate of convergence similar to that found in the Jacobi–Legendre formulation.

It has to be noted that we have used explicitly the fact that the side corresponding to $s = -1$ coincides with the symmetry axis. If, for instance, $s = 1$ is mapped onto the symmetry axis instead, then it is preferable, of course, to use the Jacobi polynomials defined by $P^{(1,0)}(s)$. These polynomials are associated with a weight function $(1 - s)$, which will go to zero for $s \to 1$. In the spectral element program used in this study the spectral elements adjacent to the symmetry axis are renumbered in such a way that the symmetry axis corresponds to the side $s = -1$ on the parent domain. Alternatively one may employ $P^{(1,0)}(s)$ polynomials when the "wrong" side is mapped onto the centerline.

If the symmetry axis coincides with $s = -1$, one can generalize the above described procedure to $P^{(\alpha,1)}(s)$ polynomials corresponding to a weight function $(1 - x)^{\alpha}(1 + x)$. This weight function will also have the property that is goes to zero in the same way as r goes to zero. Although alternative polynomials are feasible, it is not clear what the merits are of using even more general Jacobi polynomials.

The method described in this paper is generic in the sense that it can be applied to all axisymmetric (partial differential) equations. The application to the axisymmetric Stokes problem merely serves as an illustration. This particular problem has been tackled on two types of meshes. On the first mesh the grid lines are almost orthogonal to the symmetry axis and both the mixed Jacobi–Legendre method and the Legendre–Legendre method perform

equally well. On the second mesh the grid lines have been chosen to be nonorthogonal to the symmetry axis and the mixed Jacobi method gives better results than the full Legendre basis, which can be clearly seen from the convergence plots.

APPENDIX

Subroutine to Calculate the Gauss–Lobatto Points

This subroutine is essentially the one found in [1] with a minor correction in the routine JACOBF. The program is written in FORTRAN.

```
      subroutine jacobl(alpha,beta,N,xjac)
c
c  computes the Gauss-Lobatto collocation points for the
   jacobi polynomials
c
c  n:      degree of approximation
c  alpha:  parameter in jacobi weight
c  beta:   parameter in jacobi weight
c
c  xjac:   output array with the Gauss-Lobatto roots
c          they are ordered from the largest (+1.0)
           to the smallest (-1.0)
c
      implicit none
      integer N
      double precision alpha,beta,xjac(0:50)
c
      integer np,nh,npp,i,j,jm,k,kstop
      double precision pnp1p,pdnp1p,pnp,pdnp,pnm1p,pdnm1,
     $                 pnp1m,pdnp1m,pnm,pnm1m,pdnm,det,
     $                 pnm1,cs,x,pnp1,pdnp1,pn,pdn,
     $                 rp,rm,ag,bg,dth,cd,sd,ss,poly,pder,
     $                 cssave,delx,epsg,recsum,hulpar(0:64),pi
      double precision alp,bet,rv
      common /jacpar/ alp,bet,rv
      data kstop/10/
      data epsg/1.0d-25/
c
      pi = 4d0*datan(1d0)
      alp = alpha
      bet = beta
      rv = 1+alp
      np = n + 1
c
c  compute the parameters in the polynomial whose roots
   are desired
```

```
c
      call jacobf(np,pnp1p,pdnp1p,pnp,pdnp,pnm1p,pdnm1,1d0)
      call jacobf(np,pnp1m,pdnp1m,pnm,pdnm,pnm1m,pdnm1,-1d0)
      det=pnp*pnm1m-pnm*pnm1p
      rp=-pnp1p
      rm=-pnp1m
      ag=(rp*pnm1m-rm*pnm1p)/det
      bg=(rm*pnp-rp*pnm)/det
c
      xjac(1)=1d0
c     nh=(n+1)/2
      nh=n
c
c  set-up recursion relation for initial guess for the roots
c
      dth=pi/(2*n+1)
      cd=cos(2d0*dth)
      sd=sin(2d0*dth)
      cs=cos(dth)
      ss=sin(dth)
c
c  compute the first half of the roots by polynomial deflation
c
      do 39 j=2,nh
       x=cs
       do 29 k=1,kstop
         call jacobf(np,pnp1,pdnp1,pn,pdn,pnm1,pdnm1,x)
         poly=pnp1+ag*pn+bg*pnm1
         pder=pdnp1+ag*pdn+bg*pdnm1
         recsum=0d0
         jm=j-1
         do 27 i=1,jm
           recsum=recsum+1d0/(x-xjac(i))
   27    continue
         delx=-poly/(pder-recsum*poly)
         x=x+delx
         if (abs(delx).lt.epsg) goto 30
   29  continue
   30  continue
       xjac(j)=x
       cssave=cs*cd-ss*sd
       ss=cs*sd+ss*cd
       cs=cssave
   39 continue
      xjac(np)=-1d0
      npp=n+2
```

```
c
c   use symmetry for second half of the roots
c
      do 112 i=1,N+1
         hulpar(N-i+1) = xjac(i)
  112 continue
      do 113 i=0,N
         xjac(i) = hulpar(i)
  113 continue
      return
      end
c
        subroutine jacobf(n,poly,pder,polym1,pderm1,polym2,
        pderm2,x)
c
c     computes the jacobi polynomial (poly) and its derivative
c     (pder) of degree n at x
c
        implicit double precision(a-h,o-z)
        common/jacpar/alp,bet,rv
        apb = alp + bet
        poly = 1do
        pder = 0d0
        if (n.eq.0) return
        polylst = poly
        pderlst = pder
c
c  The following 2 lines differ from the ones given in [1].
c
        poly = 5d-1*(1d0+bet)*(x-1d0) + 5d-1*(1d0+alp)*(x+1d0)
        pder = 5d-1*(2d0+apb)
c
        if (n.eq.1) return
        do 19 k=2,n
          a1 = 2d0*k*(k+apb)*(2d0*k+apb-2d0)
          a2 = (2d0*k+apb-1d0)*(alp**2-bet**2)
          b3 = (2d0*k+apb-2d0)
          a3 = b3*(b3+1d0)*(b3+2d0)
          a4 = 2d0*(k+alp-1d0)*(k+bet-1d0)*(2d0*k+apb)
          polyn = ((a2+a3*x)*poly-a4*polylst)/a1
          pdern = ((a2+a3*x)*pder-a4*pderlst+a3*poly)/a1
          psave = polylst
          pdsave = pderlst
          polylst = poly
          poly = polyn
          pderlst = pder
          pder = pdern
```

```
19   contiune
     polym1 = polylst
     pderm1 = pderlst
     polym2 = psave
     pderm2 = pdsave
     return
     end
```

ACKNOWLEDGMENT

This work was supported by the Engineering and Physical Sciences Research Council of the United Kingdom under Grant No. GR/K58166 while the first author was in residence in the Department of Mathematics, University of Wales Aberystwyth, U.K.

REFERENCES

1. C. Canuto, M. Y. Hussaini, A. Quarteroni, and T. A. Zang, *Spectral Methods in Fluid Dynamics*, Springer series in Computational Physics (Springer-Verlag, Berlin/Heidelberg/London, 1987).
2. D. Funaro, *Polynomial Approximation of Differential Equations*, Lecture Notes in Physics (Springer-Verlag, Berlin, Heidelberg, 1992), Vol. m8.
3. M. I. Gerritsma and T. N. Phillips, Compatible spectral approximations for the velocity–pressure–stress formulation of the Stokes problem, *SIAM J. Sci. Comput.* **20**, 1530 (1999).
4. M. I. Gerritsma and T. N. Phillips, Discontinuous spectral element approximations for the velocity–pressure–stress formulation of the Stokes problem, *Int. J. Numer. Meth. Eng.* **43**, 1401 (1998).
5. W. J. Gordon and C. A. Hall, Construction of curvilinear coordinate systems and application to mesh generation, *Int. J. Numer. Meth. Eng.* **7**, 461 (1973).
6. W. J. Lunsmann, L. Genieser, R. C. Armstrong, and R. A. Brown, Finite element analysis of steady viscoelastic flow around a sphere in a tube: Calculations with constant viscosity models, *J. Non-Newtonian Fluid Mech.* **48**, 63 (1993).
7. Y. Maday and A.T. Patera, Spectral element methods for the incompressible Navier–Stokes equations, in *State of the Art Surveys in Computational Mechanics*, edited by A. K. Noor and J. T. Oden (ASME, New York, 1989), p. 71.
8. G. Szégo, *Orthogonal Polynomials*, American Mathematical Society Colloquium Publications (American Mathematical Society, New York, 1959), Vol. XXIII.
9. V. Van Kemenade and M. O. Deville, Application of spectral elements to viscoelastic creeping flows, *J. Non-Newtonian Fluid Mech.* **51**, 277 (1994).